Effects of uniaxial stress on orbital stripe direction in half-doped layered manganites: $Eu_{0.5}Ca_{1.5}MnO_4$ and $Pr(Sr,Ca)_2Mn_2O_7$

Y. Tokunaga,[1,2] R. Kumai,[3] N. Takeshita,[3] Y. Kaneko,[1,2] J. P. He,[1,2] T. Arima,[2,4] and Y. Tokura[1,2,3,5,6]
[1]*Multiferroics Project, ERATO, Japan Science and Technology Agency (JST), Wako, Saitama 351-0198, Japan*
[2]*Spin Superstructure Project, ERATO, JST, Tsukuba, Ibaraki 305-8562, Japan*
[3]*Correlated Electron Research Center (CERC), National Institute of Advanced Industrial Science and Technology (AIST), Tsukuba, Ibaraki 305-8562, Japan*
[4]*Institute of Multidisciplinary Research for Advanced Materials, Tohoku University, Sendai 980-8577, Japan*
[5]*Department of Applied Physics, University of Tokyo, Bunkyo-ku, Tokyo 113-8656, Japan*
[6]*Cross-Correlated Materials Research Group (CMRG), ASI, RIKEN, Wako, Saitama 351-0198, Japan*
(Received 18 July 2008; revised manuscript received 6 September 2008; published 7 October 2008)

We have studied the uniaxial-stress effects on the half-doped charge-orbital ordered (CO-OO) manganites $Eu_{0.5}Ca_{1.5}MnO_4$ and $Pr(Sr_{1-y}Ca_y)_2Mn_2O_7(y\sim0.9)$. $Eu_{0.5}Ca_{1.5}MnO_4$ with single Mn-O layer structure is ferroelastic and the application of weak uniaxial stress (<8.5 MPa) along the orbital stripe direction drives a rotation of the orbital stripes by 90° through the lattice orthorhombicity channel. For $Pr(Sr_{1-y}Ca_y)_2Mn_2O_7(y\sim0.9)$ with double Mn-O layer structure, it is revealed that the phase stability of two CO-OO states with different orbital stripe direction can be controlled by the external uniaxial pressure. In addition, the application of higher uniaxial pressure also causes a rotation of the lattice orthorhombicity itself and hence rotates the orbital stripes as well as the electric polarization axis in the low-temperature CO-OO state.

DOI: 10.1103/PhysRevB.78.155105 PACS number(s): 75.47.Lx, 81.40.Jj, 75.30.Gw, 75.47.Gk

I. INTRODUCTION

The phenomenon of charge ordering (CO) or the formation of charge stripes in transition-metal oxides such as layered-structure cuprates[1] and nickelates[2] is a central topic in the physics of correlated-electron systems. Among them, the CO in manganites is closely tied to the spin and orbital degrees of freedom of 3*d* electrons. The charge-orbital ordering (CO-OO) phenomena in manganites have been attracting much interest since its melting by application of a magnetic field causes an insulator-metal transition, one form of colossal magnetoresistance (CMR) phenomena.[3] The CO-OO in half-doped manganites is characterized by the checkerboard-type alternation of Mn^{3+}/Mn^{4+} ions and staggered-type alternation of e_g orbitals of Mn^{3+} ions, as shown in Fig. 1(b). Such an ordering pattern gives rise to anisotropic physical properties with respect to the direction of the orbital stripes (or zigzag chains) in the MnO_2 planes. In the CO-OO state, therefore, the direction in which the orbital stripes are running is an important parameter. Recent studies on single crystals of orthorhombically distorted half-doped layered and bilayered manganites have revealed that the physical properties such as optical and magnetic properties are indeed anisotropic even within the CO-OO plane.[4–6] Furthermore, a CO-OO induced electrically polar state was discovered in the bilayered compound $Pr(Sr_{1-y}Ca_y)_2Mn_2O_7(y\sim0.9)$.[5] Here, the electric polarization appears only when orbital stripes run along the *b* axis, which indicates the strong correlation between the orbital stripe direction and the electric polarization.

In the half-doped manganites with a relatively small ionic size of *A*-site cation, the deviation of the tolerance factor from the ideal value (unity) often results in the tilt of MnO_6 octahedra, hence producing a orthorhombic distortion. In these materials, the direction of orbital stripes is strongly coupled with the lattice orthorhombicity of the average structures. The coupling between the lattice orthorhombicity and the orbital stripe direction may enable us to control the orbital stripe direction by application of external mechanical stress, while conventional attempts to mechanically control the orbital state in manganites mainly aimed at changing the phase stability of orbital states by changing lattice parameters, which is accompanied by the change in spin structures as well.[7,8] In addition, $Pr(Sr_{1-y}Ca_y)_2Mn_2O_7(y\sim0.9)$ possesses two CO-OO phases with different orbital stripe directions. Since the two phases show different ratios of the lattice parameters, it is expected that one can control the orbital stripe direction also by changing relative stability between the two CO-OO states under uniaxial stress (σ). By changing the orbital stripe direction, it should also be possible to control the physical anisotropy in the CO-OO plane. Here we report the directional control of the orbital stripes by uniaxial stress in half-doped single-layered $Eu_{0.5}Ca_{1.5}MnO_4$ and bilayered $Pr(Sr_{1-y}Ca_y)_2Mn_2O_7(y\sim0.9)$.

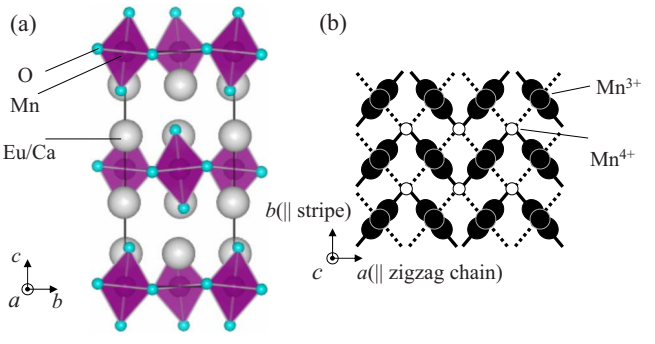

FIG. 1. (Color online) (a) Crystal structure of $Eu_{0.5}Ca_{1.5}MnO_4$. (b) Schematic of CO-OO state in a MnO_2 plane.

II. EXPERIMENT

Single crystals of $Eu_{0.5}Ca_{1.5}MnO_4$ and $Pr(Sr_{1-y}Ca_y)_2Mn_2O_7(y=0.85,0.9)$ were grown by using a floating-zone method in the atmospheres of 5 and 8 atm O_2, respectively. Single-crystal plates were cleaved off from the ingots to obtain a flat shiny *ab* plane and then cut into the rectangular shape with the widest planes perpendicular to the *c* axis. The typical dimension of the samples is $1.5\times1.0\times0.5$ mm. Temperature dependence of magnetization (M) was measured on $Eu_{0.5}Ca_{1.5}MnO_4$ and $Pr(Sr_{1-y}Ca_y)_2Mn_2O_7(y=0.9)$ single crystals under uniaxial pressures. Here, we define e_σ as the direction of uniaxial pressure. Initially e_σ was set parallel to the *b* axis (the crystallographic longer axis in the MnO_2 plane in the averaged orthorhombic unit cell) and $M\|e_\sigma$ was measured. We used a uniaxial pressure cell, which was loaded in a commercial superconducting quantum interference device (SQUID) magnetometer (MPMS, Quantum Design).[9] In order to reduce the background signal, the main body of the pressure cell is made of fiber-reinforced plastic.

The CO-OO domains were visualized by utilizing a polarization microscope with a polarizer and an analyzer set in nearly crossed Nicols positions. To check the effect of uniaxial stress visually, uniaxial stress was applied by clamping the samples with tweezers. The crystal structure including the superstructure was determined by synchrotron single-crystalline x-ray diffraction with an imaging plate (IP) system on the Beamline 1A at Photon Factory of High Energy Accelerator Research Organization (KEK), Japan. Temperature dependence of lattice parameters for $Pr(Sr_{1-y}Ca_y)_2Mn_2O_7(y=0.9)$ was determined from x-ray powder-diffraction measurements. To study the uniaxial-stress effect on the crystal structure of $Pr(Sr_{1-y}Ca_y)_2Mn_2O_7(y=0.85)$, we utilized a clamping-type uniaxial pressure cell[10] which was combined with the IP system on the Beamline 1A.

III. RESULTS AND DISCUSSIONS

A. $Eu_{0.5}Ca_{1.5}MnO_4$

$Eu_{0.5}Ca_{1.5}MnO_4$ belongs to the $n=1$ class of the Ruddlesden-Popper series composed of alternative stacking of a MnO_2 layer and a rock salt $(Eu,Ca)_2O_2$ layer [see Fig. 1(a)]. In this compound, the lattice is orthorhombically distorted from the tetragonal structure even without CO-OO because of small average radius of *A*-site cations (Eu/Ca). The orthorhombic distortion decreases the Mn-O-Mn bond angle, and thus reduces the hopping energy of the conduction electrons, and tends to stabilize the CO-OO state.[11,12] The CO-OO transition temperature (T_{CO}) is around 325 K. Space groups are *Bmab* [with $a=5.3481(5)$, $b=5.3980(6)$, and $c=11.7263(19)$ Å at 360 K] for charge-orbital disordered phase ($T>T_{CO}$), and *Pmnb* [with $a=10.6821(12)$, $b=5.4072(6)$, and $c=11.7014(19)$ Å at 290 K) for CO-OO phase ($T_{CO}>T$), respectively. The detailed structures will be published elsewhere.[13] The orthorhombic distortion of the averaged structure is characterized by the tilt of MnO_6 octahedra around the *a* axis similarly to that reported in $Pr(Sr_{1-y}Ca_y)_2Mn_2O_7(y=0.9)$. The structure above T_{CO} is isostructural with that of the so-called low-temperature orthorhombic (LTO) phase of $La_{2-x}Sr_xCuO_4$, in which a magnetic-field induced rotation of the crystallographic axis was reported.[14] The orthorhombic distortion couples with the CO-OO to determine the direction of orbital stripes in the MnO_2 plane. Below T_{CO}, orbital stripes always run along the *b* axis [see Fig. 1(b)].

Figures 2(a) and 2(b) show anisotropic in-plane reflectivity spectra cited from Ref. 4. Above T_{CO}, the reflectivity spectrum is almost isotropic [see Fig. 2(a)]. While the change in the lattice orthorhombicity caused by CO-OO in $Eu_{0.5}Ca_{1.5}MnO_4$ is subtle (change in b/a is less than 0.3%), there exists a large enhancement of the in-plane optical anisotropy below T_{CO} [Fig. 2(b)]. This is ascribed to the anisotropic transfer interaction of e_g electrons in the CO-OO plane; the transfer interaction is larger along the orbital zigzag chains than along the orbital stripes.[4] Thus, one can visualize the orbital stripe direction by utilizing a polarization microscope. The band-shaped domains are visible in $Eu_{0.5}Ca_{1.5}MnO_4$ with weak bright-and-dark contrasts even above T_{CO} in the polarization microscope image (not shown). This is because the lattice is orthorhombic even above T_{CO} and shows a slight optical anisotropy. Observed domains correspond to structural twins with different *a*-axis directions by 90° from each other. No additional texture appears in the polarization microscope images while cooling the sample through T_{CO}, while the contrast is strongly enhanced. This means that the orthorhombic twin domains coincide with those of CO-OO domains, suggesting the clamping between the lattice orthorhombicity and the stripe direction in the CO-OO state in this compound.

Figure 2(c) shows a polarization microscope image of a cleaved surface (*ab* plane) at room temperature (below T_{CO}). Most part of the crystal shows bright color, while minority twin domains appear as narrow dark bands running along diagonal direction of the image. The *b* axis or the stripe direction of the majority domains is indicated by a white arrow in Fig. 2(c). Figure 2(d) shows a polarization microscope image recorded after the application of uniaxial stress along the *b* axis or the orbital stripe direction of the majority domains in Fig. 2(c) with the use of a pair of tweezers. The change in the brightness suggests that the stripe direction is rotated by 90° so as to be aligned perpendicular to the direction of the stress. The change was confirmed to be reversible, for example, when uniaxial stress is applied perpendicular to the stress direction shown in Fig. 2(d), domains with bright color become dominant. A similar phenomenon is also observed above T_{CO} although the contrast is much reduced. This fact indicates that $Eu_{0.5}Ca_{1.5}MnO_4$ is ferroelastic as is characterized by the existence of two energetically degenerate states (domains) with commutativity by the application of external stress.[15] In the absence of external stress, elastic energies of these domains are equivalent. When uniaxial stress is applied along the *a* or *b* axis, the degeneracy of directional freedom of spontaneous strain is lifted so as to align the shorter axis, i.e., the *a* axis, along the stress direction. Thus, domain boundaries move so as to expand domains with the *a* axis along the direction of the stress. Below T_{CO}, because of the clamping between orbital stripe direction

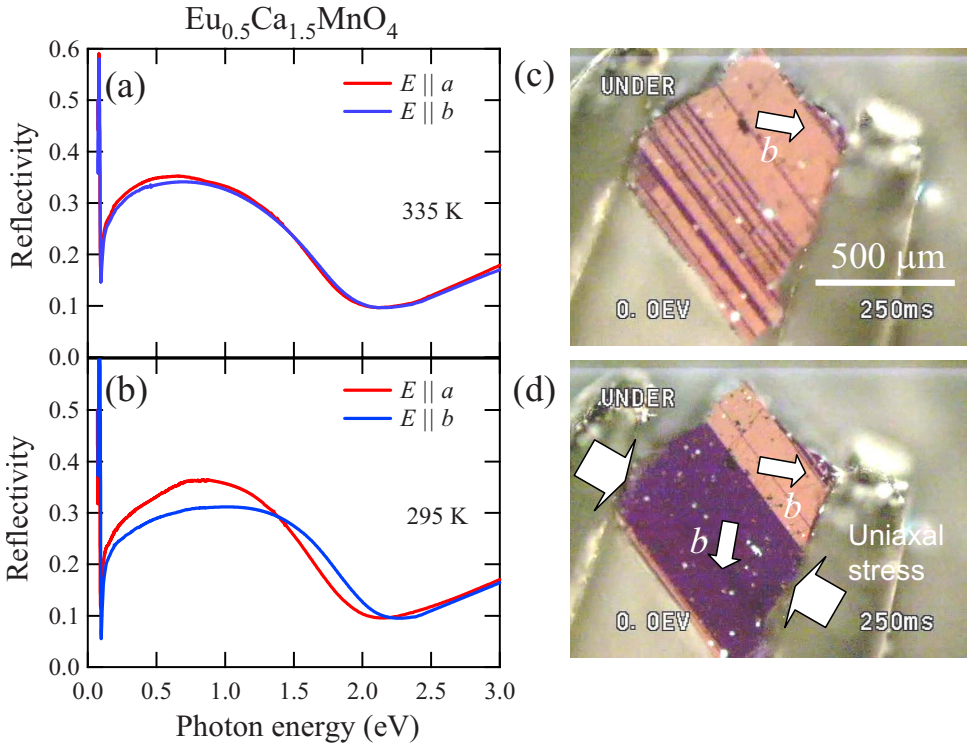

FIG. 2. (Color online) (a) and (b) Light polarization dependence of reflectivity spectra for $Eu_{0.5}Ca_{1.5}MnO_4$ measured at (a) $T=335$ K ($T>T_{CO}$) and (b) $T=295$ K ($T<T_{CO}$) (cited from Ref. 4). (c) and (d) Polarizing microscope images of a cleaved surface (*ab* plane) of $Eu_{0.5}Ca_{1.5}MnO_4$ taken at room temperature (c) before and (d) after the application of uniaxial stress. The direction of the uniaxial stress is indicated by thick white arrows.

and lattice orthorhombicity, orbital stripes also rotate with the lattice orthorhombicity as external stress is applied along the *b* axis. Note that other physical properties such as magnetization along the *a* and *b* axes are also exchangeable by the application of weak stress.

Figure 3 shows the temperature dependence of magnetization along the *a* and *b* axes with or without uniaxial pressure. The temperature dependence of anisotropic magnetization measured without uniaxial pressure suggests the antiferromagnetic transition at around 120 K and that the magnetic easy axis is the *b* axis (or the orbital stripe direction). It is interesting to note that the directional relation among the tilt of MnO_6 octahedra, the orbital stripe, and the easy axis below T_N is the same as that reported in orthorhombic perovskite $Pr_{0.5}Sr_{0.4}Ca_{0.1}MnO_3$ (Ref. 16) and the CO2 (lower-temperature CO) phase of bilayered compound $Pr(Sr_{0.1}Ca_{0.9})_2Mn_2O_7$;[5] in both cases the orthorhombicity of the averaged unit cell simply comes from tilt of MnO_6 octahedra without rotation, similarly to the case of $Eu_{0.5}Ca_{1.5}MnO_4$. While applying external stress of 8.5 MPa along the *b* axis, the slope of magnetization $M \| e_\sigma$ below T_N increases and comes close to that along the *a* axis (see a dashed line in Fig. 3), signaling a rotation of the easy axis while keeping T_N and T_{CO} intact. Further increase in stress hardly affects the magnetization. This suggests that the application of uniaxial pressure of as low as 8.5 MPa is enough to overcome a ferroelastic coercive stress, to exchange the *a* and *b* axes, and thus to change the orbital stripe direction in the CO-OO phase. Thus, we have demonstrated that the application of relatively small uniaxial stress drives a rotation of orbital stripe direction and accordingly the CE-type zigzag spin chain direction by 90° in the CO-OO state for $Eu_{0.5}Ca_{1.5}MnO_4$.

B. $Pr(Sr_{1-y}Ca_y)_2Mn_2O_7(y\sim0.9)$

$Pr(Sr_{1-y}Ca_y)_2Mn_2O_7(y\sim0.9)$ belongs to the $n=2$ compound of the Ruddlesden-Popper series composed of alternative stacking of a double MnO_2 layer and a rock salt layer [see Fig. 4(a)]. As already reported,[5] $Pr(Sr_{1-y}Ca_y)_2Mn_2O_7(y\sim0.9)$ is crystallized in an orthorhombically distorted form even above T_{CO}. There exist two types of CO-OO phases: the high-temperature CO1 phase and the low-temperature CO2 phase. Orbital stripes run along the *a* axis in the CO1 phase while along the *b* axis in the CO2 phase. The space groups are *Amam* (with $a=5.410$, $b=5.462$, and $c=19.277$ A at 405 K) for the charge disordered phase ($T>T_{CO1}$), *Pbnm* (with $a=5.412$, $b=10.921$, and $c=19.234$ A at 330 K) for the CO1 ($T_{CO1}>T>T_{CO2}$), and *Am2m* (with $a=10.812$, $b=5.475$, and $c=19.203$ A at 295 K) for the CO2 ($T<T_{CO2}$). A recent study on $Pr(Sr_{1-y}Ca_y)_2Mn_2O_7$ system has revealed that the existence of the CO1 phase is limited only well above T_N.[17] This implies some role of the spin correlation developed with lowering temperature below T_{CO1} in inducing the rotational transition of orbital stripes. Asymmetric deformations of MnO_6 octahedra along the *c* axis which is unique to the bilayered system as well as its influence on the ordered orbital shapes of e_g electrons may also has some relevance,[13] while its detailed mechanism is to be clarified in the future study. It is noted that in the CO2 phase the electric polariza-

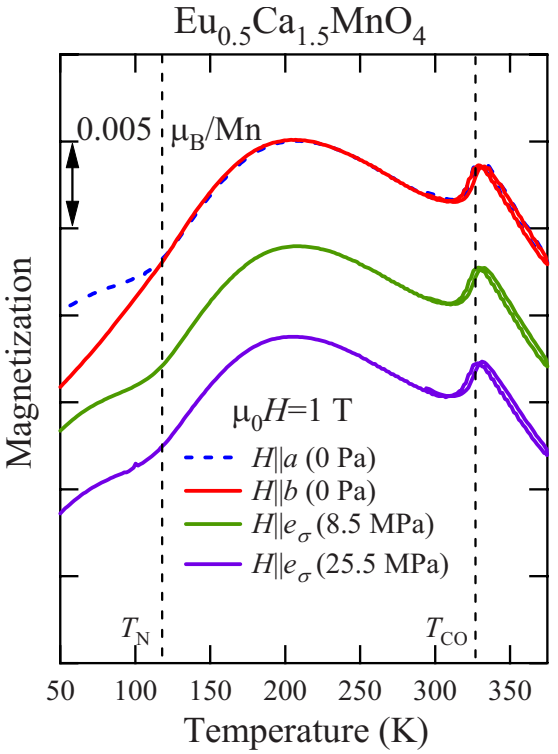

FIG. 3. (Color online) Temperature dependence of magnetization of $Eu_{0.5}Ca_{1.5}MnO_4$ along the a axis (a dashed line) and the b axis (solid lines) measured with or without existence of uniaxial pressure. e_σ was initially set along the b axis and $M\|e_\sigma$ is measured at uniaxial pressures of 8.5 and 20.5 MPa (solid lines). The background signals from the pressure cell are subtracted.

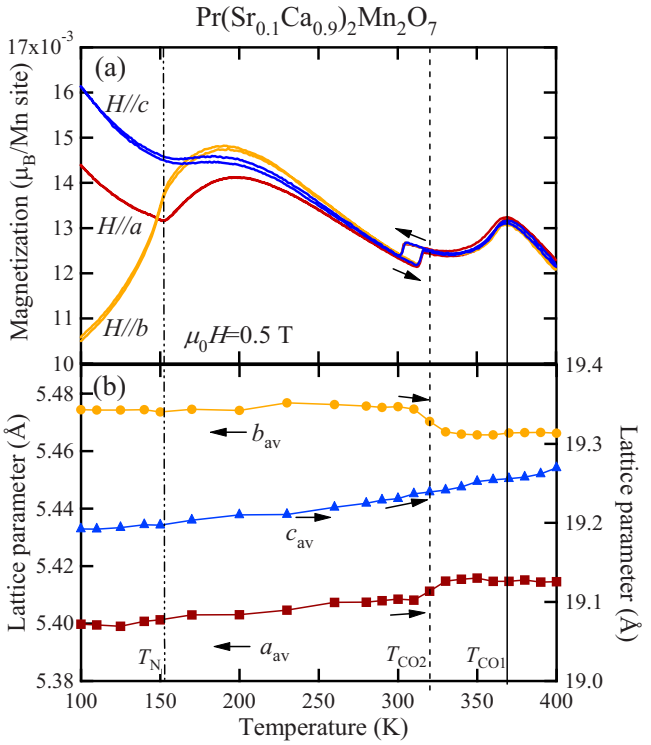

FIG. 5. (Color online) Temperature dependence of (a) magnetization cited from Ref. 5 and (b) lattice parameters of $Pr(Sr_{1-y}Ca_y)_2Mn_2O_7(y\sim0.9)$.

tion directs toward the b axis, i.e., the orbital stripe direction.

Figure 5 shows temperature dependence of magnetization cited from Ref. 5 and the averaged lattice parameters a_{av}, b_{av}, and c_{av} (in the orthorhombic *Amam* setting of the $T>T_{CO1}$ phase) of $Pr(Sr_{1-y}Ca_y)_2Mn_2O_7(y=0.9)$. Note that the b axis

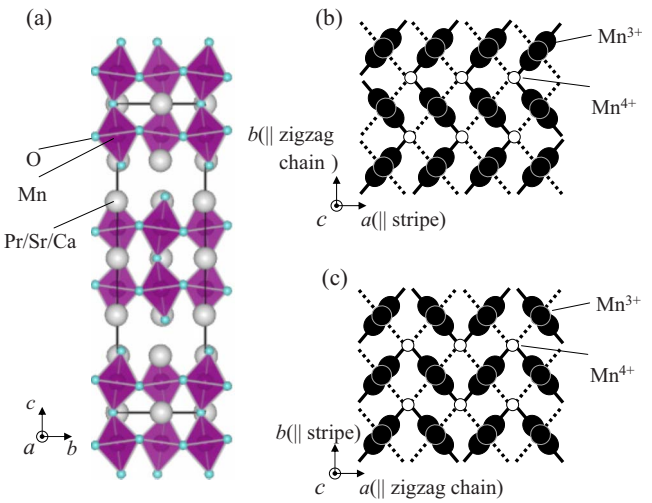

FIG. 4. (Color online) (a) Crystal structure of $Pr(Sr_{1-y}Ca_y)_2Mn_2O_7(y\sim0.9)$. (b) and (c) Schematics of the CO-OO states in a MnO_2 plane for the (b) CO1 and (c) CO2 phases of $Pr(Sr_{1-y}Ca_y)_2Mn_2O_7(y\sim0.9)$.

(the longer axis of the averaged structure) is doubled in the CO1 phase ($b=2b_{av}$) and the a axis (the shorter axis of the averaged structure) is doubled in CO2 phase ($a=2a_{av}$). The magnetization shows a large anisotropy between the a- and b-axis components. The b axis (parallel to the orbital stripe) is the magnetic easy axis. On warming, a_{av} expands and b_{av} shrinks at T_{CO2}, while they change little at T_{CO1} and T_N. The c_{av} increases monotonically as temperature increases.

Figures 6 shows uniaxial-stress dependence of M-T curves for $Pr(Sr_{1-y}Ca_y)_2Mn_2O_7(y=0.9)$. Stresses with various strengths were initially applied along the b axis and then M along e_σ was measured. As the stress increases, the slope of M below T_N changes from positive to negative similarly to the case of $Eu_{0.5}Ca_{1.5}MnO_4$ while the T_N value hardly changes. This suggests the change in the magnetic easy axis by the application of uniaxial pressure. The centroid position of the hysteresis at T_{CO2} first shifts toward lower temperature for $\sigma\leq40$ MPa, then moved back toward higher temperature as the stress further increases, while the T_{CO1} value does not change. In Fig. 7, we plot uniaxial-stress dependence of T_{CO1}, T_{CO2}, and T_N. Although the T_{CO2} value is strongly influenced by the application of uniaxial stress, T_{CO1} and T_N hardly change. This is consistent with the fact that the change in the lattice parameters across T_{CO1} and T_N is small (see Fig. 5).

The main difference from the case of $Eu_{0.5}Ca_{1.5}MnO_4$ is the existence of two CO-OO phases with different orbital stripe directions. Since the two phases show different ratios of the lattice parameters a_{av} and b_{av}, the relative stability between two CO-OO states can be modified with the uniaxial stress. The ratio a_{av}/b_{av} in the CO1 is larger than that in the

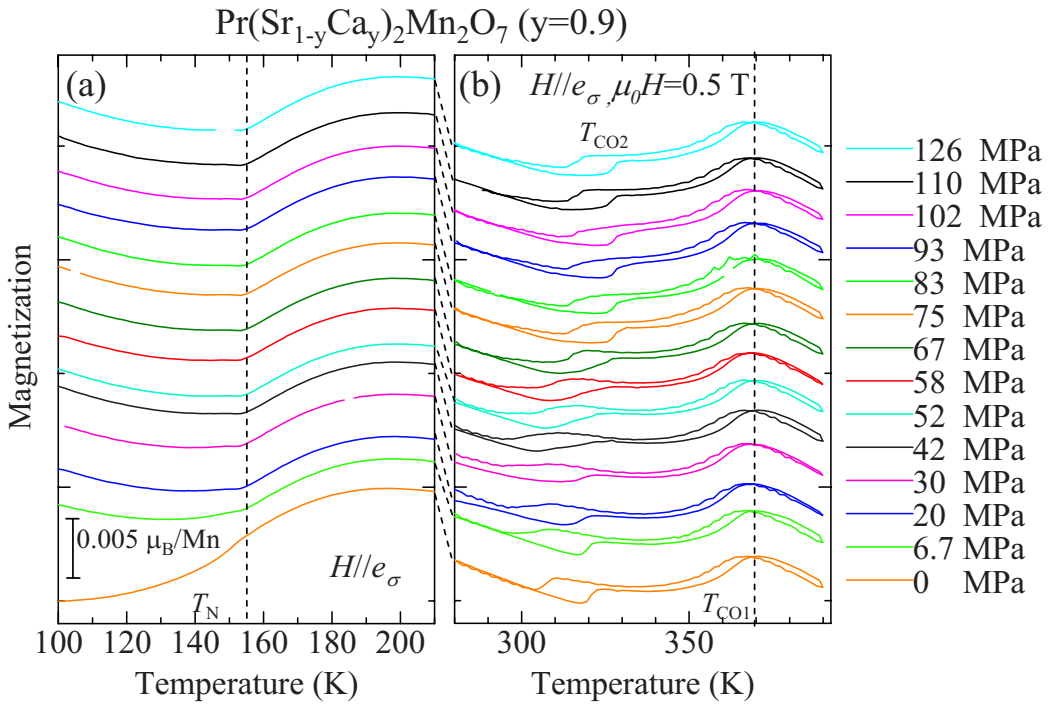

FIG. 6. (Color online) Uniaxial-stress dependence of M-T curves at around (a) T_{CO2} and (b) T_N for $Pr(Sr_{1-y}Ca_y)_2Mn_2O_7(y\sim0.9)$. e_σ was initially set along the b axis and $M\|e_\sigma$ is measured.

CO2. Thus, the application of uniaxial stress along the b axis is expected to stabilize the CO1 phase against the CO2 phase. However, if the system has ferroelastic nature and stress is large enough to overcome the coercive stress, a rotation of orthorhombicity may occur similarly to the case of $Eu_{0.5}Ca_{1.5}MnO_4$ and the a and b axes may be exchanged. In such a case, the stress will work so as to shorten the a axis, thus stabilize the CO1 in turn. The increasing tendency of T_{CO2} for $\sigma\geq\sim40$ MPa is consistent with this scenario. Such a situation is summarized in a schematic temperature (T) uniaxial pressure (σ) phase diagram of $Pr(Sr_{1-y}Ca_y)_2Mn_2O_7(y\sim0.9)$ in Fig. 8. At around T_{CO2}, four types of domains, i.e., domains of CO1, CO2, and their crystallographically equivalent twins, are nearly degenerate in energy in the absence of external stress. The degeneracy can be lifted by the application of a uniaxial stress. When a uniaxial stress is applied along the b axis (i.e., the longer axis of the averaged unit cell) in the CO2 phase at around T_{CO2}, CO1 domains nucleate and expand without changing the b direction. With further increasing σ to overcome the ferroelastic coercive force, the exchange of the a and b directions occurs. The CO2 phase is more stabilized than the CO1 phase by such a strong uniaxial stress along the a axis. As a consequence, the change occurs in a manner of CO2 $\rightarrow$CO1$\rightarrow$CO2 concomitantly with the change in $e_\sigma\|b\|$stripe$\rightarrow e_\sigma\|b\perp$ stripe$\rightarrow e_\sigma\|a\perp$ stripe, as indicated with a dash-dotted arrow in Fig. 8. Such changes are in fact confirmed by x-ray diffraction measurements. Figure 9 shows uniaxial-stress dependence of the lattice parameters and selected areas of x-ray oscillation photographs at $T=295$ K. The $y=0.85$ compound at $T=295$ K is in the thermal hysteresis of the phase transition from the CO1 to CO2 phase. The sample was first cooled to ~270 K and slowly warmed to

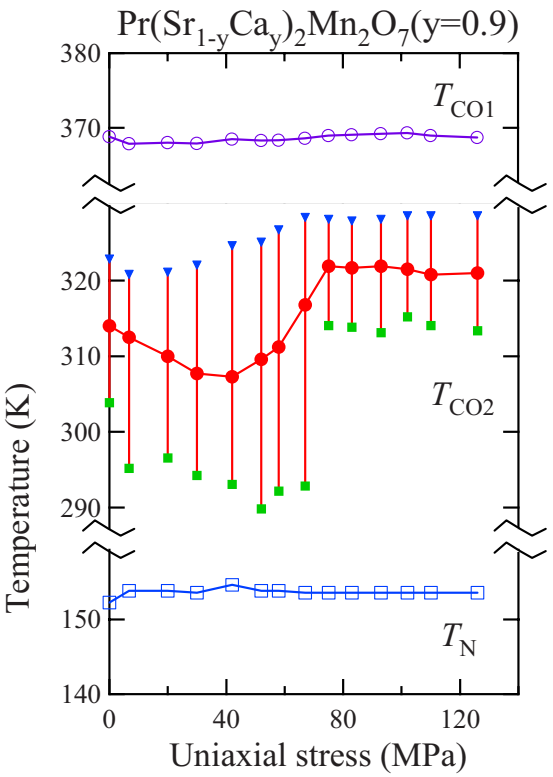

FIG. 7. (Color online) Uniaxial-stress dependence of T_{CO1}, T_{CO2}, and T_N for $Pr(Sr_{1-y}Ca_y)_2Mn_2O_7(y\sim0.9)$. Filled circles indicate the centroid positions of thermal hystereses at T_{CO2}. Filled squares and triangles indicate T_{CO2} determined from cooling and warming branch of magnetization.

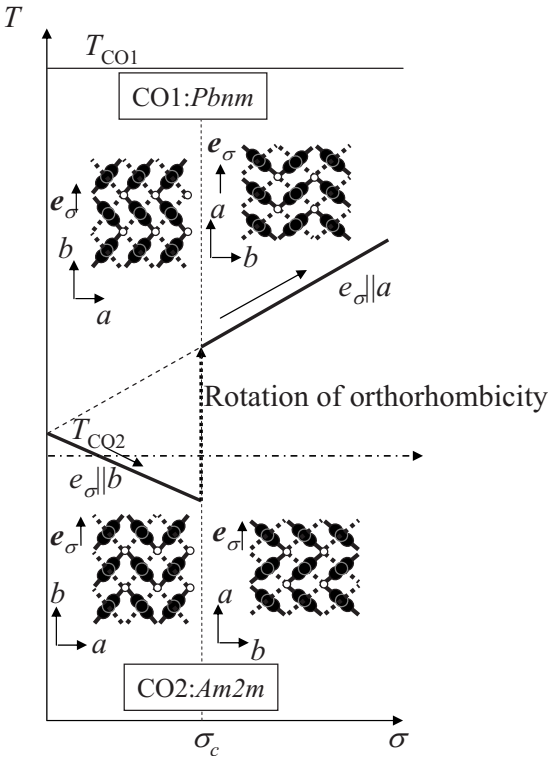

FIG. 8. Schematic of structural phase diagram for $Pr(Sr_{1-y}Ca_y)_2Mn_2O_7(y\sim0.9)$. Initially, e_σ was set along the b axis. As uniaxial stress (σ) increases and becomes larger than ferroelastic coercive stress σ_c, the a and b axes of the averaged structure are exchanged. Thus, the e_σ direction changes to along the a axis.

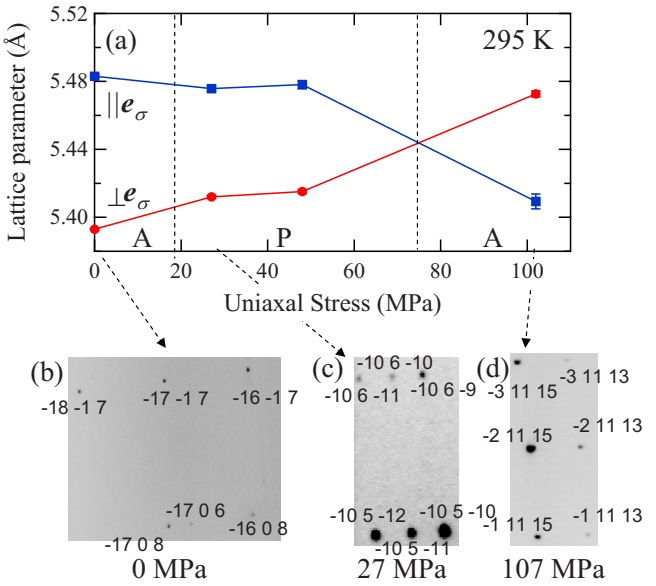

FIG. 9. (Color online) (a) Uniaxial-stress dependence of in-plane lattice parameters measured for $Pr(Sr_{1-y}Ca_y)_2Mn_2O_7(y=0.85)$ at 295 K. (b)–(d) Imaging plate images of the selected areas of x-ray diffraction taken at (b) $\sigma=0$ MPa (indexed by *Am2m* setting including superstructure), (c) 27 MPa (indexed by *Pbnm* setting including superstructure), and (d) 108 MPa (indexed by *Am2m* setting including superstructure), respectively. Existence of *hkl* reflection with $k+l=2m+1$ in (c) suggests the disappearance of A-centered structure.

295 K so as to be in the CO2 state. Uniaxial pressure (σ) was initially applied along the b axis ($e_\sigma \| b$) and gradually increased. No reflection at *hkl* with $k+l=2m+1$(m:integer) is observed at the ambient pressure [see Fig. 9(b)], indicating the A-centered structure consistent with the space group of the CO2 phase. On applying uniaxial pressure of 27 MPa, reflections with $k+l=2m+1$ emerge [see Fig. 9(c)], accompanied by a rotation of the positions of superlattice spots by 90° while keeping the relation among lattice parameters of the averaged unit cell intact. This means that the CO2 phase is destabilized by the application of uniaxial stress and the lattice structure changes to the primitive one of the CO1 phase. Further increase in uniaxial stress ($\sigma \leq 107$ MPa) changes the lattice parameter along the stress direction to the shorter one, indicating the exchange between the a and b axes of the averaged unit cell. At the same time, the A-centered structure is recovered [see Fig. 9(d)], suggesting that the phase re-enters the CO2.

As shown above, $Pr(Sr_{1-y}Ca_y)_2Mn_2O_7(y\sim0.9)$ is ferroelastic as well as antiferromagnetic and electrically polar and hence may be considered as a *multiferroic*. This compound has a large in-plane anisotropy in optical and magnetic responses because of the CO-OO and one can control the physical properties by uniaxial stress through the coupling between the orbital arrangement and the lattice orthorhombicity.

IV. SUMMARY

We have studied the uniaxial-stress effect on the half-doped charge-orbital ordered (CO-OO) manganites $Eu_{0.5}Ca_{1.5}MnO_4$ and $Pr(Sr_{1-y}Ca_y)_2Mn_2O_7(y\sim0.9)$. It is shown that $Eu_{0.5}Ca_{1.5}MnO_4$ is ferroelastic and the application of weak uniaxial stress (<8.5 MPa) along the orbital stripe direction drives a rotation of the orbital stripes by 90° together with the lattice orthorhombicity. For $Pr(Sr_{1-y}Ca_y)_2Mn_2O_7(y\sim0.9)$, it is shown that the phase stability of two CO-OO states with different orbital stripe directions can be controlled by external uniaxial pressure. In addition, the application of a higher uniaxial pressure also causes a switching of the lattice orthorhombicity itself and thus rotates the orbital stripe direction as well as the electric polarization axis in the low-temperature polar CO-OO state.

ACKNOWLEDGMENTS

The authors thank M. Uchida, D. Okuyama, and Y. Taguchi for fruitful discussions and Y. S. Lee for providing the reflectivity data. This work was in part supported by Grant-in-Aids for Scientific Research from the MEXT, Japan (Grants No. 20340086, No. 16076205, and No. 19340089).

[1] J. M. Tranquada, B. J. Sternlieb, J. D. Axe, Y. Nakamura, and S. Uchida, Nature (London) **375**, 561 (1995).
[2] J. M. Tranquada, D. J. Buttrey, V. Sachan, and J. E. Lorenzo, Phys. Rev. Lett. **73**, 1003 (1994).
[3] Y. Tokura, Rep. Prog. Phys. **69**, 797 (2006).
[4] Y. S. Lee, S. Onoda, T. Arima, Y. Tokunaga, J. P. He, Y. Kaneko, N. Nagaosa, and Y. Tokura, Phys. Rev. Lett. **97**, 077203 (2006).
[5] Y. Tokunaga, Th. Lottermoser, Y. S. Lee, R. Kumai, M. Uchida, T. Arima, and Y. Tokura, Nature Mater. **5**, 937 (2006).
[6] Y. S. Lee, Y. Tokunaga, T. Arima, and Y. Tokura, Phys. Rev. B **75**, 174406 (2007).
[7] Y. Konishi, Z. Fang, M. Izumi, T. Manako, M. Kasai, H. Kuwahara, M. Kawasaki, K. Terakura, and Y. Tokura, J. Phys. Soc. Jpn. **68**, 3790 (1999).
[8] T. H. Arima and K. Nakamura, Phys. Rev. B **60**, R15013 (1999).
[9] N. Takeshita, T. Sasagawa, T. Sugioka, Y. Tokura, and H. Takagi, J. Phys. Soc. Jpn. **73**, 1123 (2004).
[10] T. Hasegawa, R. Kumai, Y. Takahashi, Y. Tokura, and H. Sawa, Rev. Sci. Instrum. **76**, 073903 (2005).
[11] M. Ibarra, R. Retoux, M. Hervieu, C. Autret, A. Maignan, C. Martin, and B. Raveau, J. Solid State Chem. **170**, 361 (2003).
[12] R. Mathieu, M. Uchida, Y. Kaneko, J. P. He, X. Z. Yu, R. Kumai, T. Arima, Y. Tomioka, A. Asamitsu, Y. Matsui, and Y. Tokura, Phys. Rev. B **74**, 020404(R) (2006).
[13] D. Okuyama, Y. Tokunaga, R. Kumai, Y. Taguchi, T. Arima, and Y. Tokura, (unpublished).
[14] A. N. Lavrov, S. Komiya, and Y. Ando, Nature (London) **418**, 385 (2002).
[15] K. Aizu, J. Phys. Soc. Jpn. **27**, 387 (1969).
[16] Z. Jirák, F. Damay, M. Hervieu, C. Martin, B. Raveau, G. André, and F. Bourée, Phys. Rev. B **61**, 1181 (2000).
[17] Y. Tokunaga, T. J. Sato, M. Uchida, R. Kumai, Y. Matsui, T. Arima, and Y. Tokura, Phys. Rev. B **77**, 064428 (2008).